Monomeric Magnesium and Calcium Complexes Containing the Bidentate, Dianionic 1,2-Bis[(2,6-diisopropylphenyl)imino]acenaphthene Ligand

Igor L. Fedushkin,*[a] Alexandra A. Skatova,[a] Valentina A. Chudakova,[a] Georgy K. Fukin,[a] Sebastian Dechert,[b] and Herbert Schumann*[b]

Dedicated to Prof. Irina P. Beletskaya on occasion of her anniversary

Keywords: Magnesium / Calcium / N ligands / Anions / Dianions

The reduction of 1,2-bis[(2,6-diisopropylphenyl)imino]-acenaphthene (2,6-*i*Pr$_2$C$_6$H$_3$-BIAN) with metallic magnesium or calcium in THF affords the monomeric complexes (2,6-*i*Pr$_2$C$_6$H$_3$-BIAN)Mg(THF)$_3$ (**1**) and (2,6-*i*Pr$_2$C$_6$H$_3$-BIAN)-Ca(THF)$_4$·(THF)$_{1/2}$ (**2**). The crystallisation of **1** and **2** from benzene causes the removal of one of the coordinated THF molecules, yielding (2,6-*i*Pr$_2$C$_6$H$_3$-BIAN)Mg(THF)$_2$·(C$_6$H$_6$)$_{1/2}$ (**3a**) and (2,6-*i*Pr$_2$C$_6$H$_3$-BIAN)Ca(THF)$_3$ (**4**). Repeated recrystallisation of **1** from benzene gives (2,6-*i*Pr$_2$C$_6$H$_3$-BIAN)Mg(THF)$_2$·(C$_6$H$_6$)$_2$ (**3b**). Although the crystals of **3a** and **3b** differ in colour and in their crystallographic parameters, their molecular dimensions are very similar. Recrystallisation of **1** from pyridine produces (2,6-*i*Pr$_2$C$_6$H$_3$-BIAN)Mg(py)$_3$·(py)$_2$ (**5**). Complexes **1**–**5** have been characterised by elemental analysis, UV, IR and ^{1}H NMR spectroscopy, as well as by single-crystal X-ray diffraction.

Introduction

The first reports on the preparation of bis(arylimino)acenaphthenes (Ar-BIAN) were published in the late sixties.[1] However, the complex chemistry of these ligands was not explored before the early nineties, when van Asselt and Elsevier reported in a series of papers on the synthesis and application of Ar-BIAN complexes.[2] In the last decade, Ar-BIAN complexes of the transition metals, mainly of the late transition metals, have been studied extensively[3−7] due to the wide range of their applications, for example in the catalytic hydrogenation of alkynes,[3] C−C[4] and C−Sn[5] bond formation, and especially in olefin polymerisation.[6] While metal complexes containing radical-anionic or -dianionic ligands generated by reduction of 2,2′-bipyridyl[8] or of diimines like 1,4-diaza-1,3-dienes (DAD)[9] are well-known, investigations concerning Ar-BIAN were unknown until now. However, it is to be supposed that Ar-BIAN will be easily reduced forming not only radical-monoanions or -dianions, but also radical-trianions or even -tetraanions, since these ligands can be considered as hybrids of naphthalene and diazadienes, components which either can be reduced to radical-anions and -dianions (Scheme 1). Thus, several metal complexes with DAD[9f−9i] or naphthalene[10] dianions have been previously reported. According to the reduction potentials of acenaphthylene (−1.63 V),[11] 1,4-di-*tert*-butyl-1,4-diaza-1,3-diene (−1.82 V),[12] and naphthalene (−2.6 V),[11] the alkali metals lithium, sodium, or potassium, possessing reduction potentials of −3.05, −2.71, or −2.92 V,[13] respectively, should be suitable for the reduction of Ar-BIAN ligands. Actually, we were able to synthesise and to determine the structures

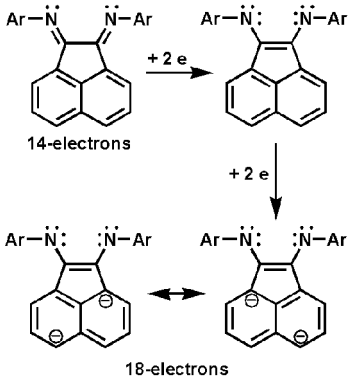

Scheme 1

[a] G. A. Razuvaev Institute of Organometallic Chemistry of Russian Academy of Sciences
Tropinina 49, 603950 Nizhny Novgorod GSP-445, Russia
Fax: (internat.) +7-8312/661-497
E-mail: igorfed@imoc.sinn.ru
[b] Institut für Chemie der Technischen Universität Berlin
Straße des 17. Juni 135, 10623 Berlin, Germany
Fax: (internat.) +49-(0)30/3142-2168
E-mail: schumann@chem.tu-berlin.de

  DOI: 10.1002/ejic.200300181

of the sodium salts of the mono-, di-, tri- and tetraanions of Ar-BIAN.[14]

In this paper, we report on the products obtained by the reduction of 2,6-*i*$Pr_2C_6H_3$-BIAN with metallic magnesium and calcium. In this context the successful synthesis of heteroleptic magnesium β-diketiminato complexes,[15] homoleptic alkaline-earth bis-β-diketiminates,[16] and alkaline-earth metal complexes containing diazadiene ligands[17–19] should be mentioned.

Results and Discussion

(2,6-*i*$Pr_2C_6H_3$-BIAN)$Mg(THF)_3$ (1) and (2,6-*i*$Pr_2C_6H_3$-BIAN)$Ca(THF)_4\cdot(THF)_{1/2}$ (2)

The reduction of 2,6-*i*$Pr_2C_6H_3$-BIAN by activated metallic magnesium or calcium in THF affords the complexes (2,6-*i*$Pr_2C_6H_3$-BIAN)$Mg(THF)_3$ (**1**) and (2,6-*i*$Pr_2C_6H_3$-BIAN)$Ca(THF)_4\cdot(THF)_{1/2}$ (**2**), each in high yield.

(2,6-*i*$Pr_2C_6H_3$-BIAN) + M $\xrightarrow{\text{THF}}$ (2,6-*i*$Pr_2C_6H_3$-BIAN)$M(THF)_n\cdot(THF)_x$

1, 2

1 M = Mg, $n = 3$, $x = 0$

2 M = Ca, $n = 4$, $x = 1/2$

The reactions require the use of an excess of the respective metal, the activation of the metal shavings or granules, and a short reflux of the reaction mixture. The activation of the metals can be achieved by the addition of CH_2I_2 or CH_3I. The presence of the diiodides in a molar amount similar to that of the ligand causes the intermediate formation of the mixed ligand complexes (2,6-*i*$Pr_2C_6H_3$-BIAN)$MI(THF)_n\cdot(THF)_x$ (M = Mg, Ca), which, however, on refluxing the reaction mixtures react with the respective metal being present in excess to give **1** or **2**. In our experiments, we used CH_2I_2 to activate the metals. The formation of species in which the metals are coordinated to two 2,6-*i*$Pr_2C_6H_3$-BIAN radical anions has not been observed. The preferential formation of **1** and **2** is confirmed by the fact that the isolated complexes do not react further with the free ligand in THF. Nevertheless, it is to be expected that such complexes will be formed under changed conditions and, very recently, we successfully synthesised and characterised the solvent-free homoleptic complexes (2,6-*i*$Pr_2C_6H_3$-BIAN)$_2$M (M = Mg, Ca).[20] Complex **2** can also be prepared by reacting K_2(2,6-*i*$Pr_2C_6H_3$-BIAN) in situ with CaI_2 in THF or by reduction of 2,6-*i*$Pr_2C_6H_3$-BIAN with calcium naphthalenide, $(C_{10}H_8)Ca(THF)_2$, but its synthesis starting from pure calcium metal proved to be the most convenient method for laboratory use.

At the temperature of refluxing THF, the reaction mixtures show a green (**1**) or green-brown colour (**2**) and the time at which the colour of the mixtures does not become more intense can be considered as the end of the reactions. On cooling the mixtures below 0 °C, their colour turns to red-brown.

Both compounds crystallise from concentrated THF solutions as block-like, deep-red crystals, which are highly sensitive towards oxygen and water. In addition to the 2,6-*i*$Pr_2C_6H_3$-BIAN ligand, THF molecules complete the coordination sphere of the metal atoms. Owing to the difference in the ionic radii of the cations, three THF molecules are coordinated to the Mg^{II} cation in **1** and four THF molecules to the Ca^{II} cation in **2**.

In the ^{1}H NMR spectrum of **1**, the methyl protons of the four isopropyl groups give rise to two doublets centred at δ = 1.16 and 1.03 ppm due to the restricted rotation of the 2,6-*i*$Pr_2C_6H_3$ groups and the methine protons appear as a septet at δ = 3.85 ppm. All the aromatic protons appear as a broad signal at δ = 4.5 to 8.0 ppm with only four peaks, one of them showing a spin-spin coupling structure (doublet at δ = 6.81 ppm). The broadening of these signals may be explained by a dynamic process in the coordination sphere of the metal associated with an equilibrium between complex molecules with three or two coordinated THF ligands (Scheme 2). The assumption of such a dynamic process seems to be justified by the molecular structure of **1**, which shows that one of the three Mg-O_{THF} bonds is significantly longer than the other two (see Figure 2).

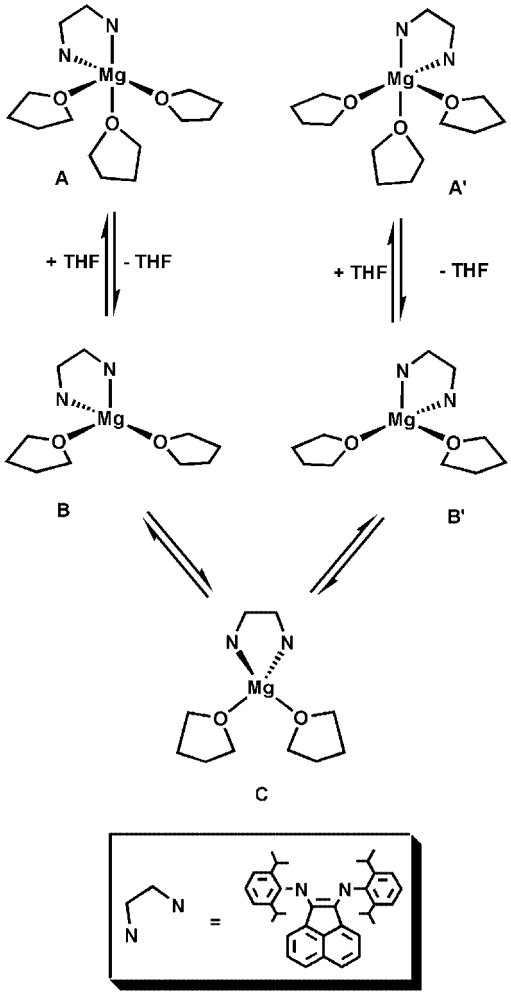

Scheme 2

The IR spectra of the complexes **1** and **2** confirm the dianionic character of the 2,6-*i*$Pr_2C_6H_3$-BIAN ligand. The strongest absorptions in the IR spectrum of the free ligand are the C=N stretching vibrations at 1671, 1652, and 1642 cm^{-1}.[7a,7b] In the Cu^I complex [(2,6-*i*$Pr_2C_6H_3$-BIAN)-$CuBr]_2$ in which the 2,6-*i*$Pr_2C_6H_3$-BIAN ligand acts as a neutral bidentate ligand, the corresponding absorptions are shifted only slightly to lower wavenumbers (1669 and 1633 cm^{-1}),[7a,7b] whereas these vibrations are totally absent in the spectra of **1** and **2** which show the C-N stretching vibration at ca. 1300 cm^{-1} (broad band) as the most intensive absorption associated with the 2,6-*i*$Pr_2C_6H_3$-BIAN ligand.

(2,6-*i*$Pr_2C_6H_3$-BIAN)$Mg(THF)_2\cdot(C_6H_6)_n$ [$n = 0.5$ (**3a**), $n = 2$ (**3b**)] and (2,6-*i*$Pr_2C_6H_3$-BIAN)$Ca(THF)_3$ (**4**)

The starting point of our research on magnesium and calcium Ar-BIAN complexes was the preparation of coordinatively unsaturated, highly reactive complexes. In the case of the coordinatively saturated complexes **1** and **2**, this corresponds to the elimination of coordinated THF ligands. Several methods are known to eliminate coordinated solvent molecules from metal complexes, including the sublimation of the compounds in high vacuum or the distillation of solutions of the compounds in non-coordinating media. Since initial attempts to eliminate THF molecules from **1** or **2** by heating the complexes in vacuo up to 180 °C failed, we used the "wet" method. Crude **1** and **2**, dried in vacuo, were dissolved in benzene forming green solutions which were heated to 60−80 °C. Cooling of these solutions to ambient temperature resulted in the separation of khaki-coloured cubic crystals when starting from **1** or of red prismatic crystals when starting from **2**. The ratio of the THF protons to the methyl protons of the 2,6-*i*$Pr_2C_6H_3$-BIAN ligand, estimated by integration of the respective ^1H NMR signals, indicates that both **1** and **2** lost one THF ligand in the course of this dissolution-crystallisation procedure, thus changing into (2,6-*i*$Pr_2C_6H_3$-BIAN)$Mg(THF)_2\cdot(C_6H_6)_{1/2}$ (**3a**) and (2,6-*i*$Pr_2C_6H_3$-BIAN)$Ca(THF)_3$ (**4**). In the case of **1**, the repetition of this procedure again leads to a different complex, the emerald-green, rhombic crystals of (2,6-*i*$Pr_2C_6H_3$-BIAN)$Mg(THF)_2\cdot(C_6H_6)_2$ (**3b**). Complex **3b** differs from **3a** only in the number of C_6H_6 lattice molecules. Surprisingly, crystallisation of **3b** from benzene again affords crystals of different colour and shape: thin, square, deep-brown coloured plates (**3c**). The NMR spectrum of **3c** is almost identical to that of **3b** and indicates the presence of two THF molecules coordinated to the magnesium. Unfortunately, the crystals of **3c** were not suitable for X-ray diffraction. However, based on the data of the crystal structures of **3a** and **3b**, one can suggest that **3c** differs from **3a** and **3b** only with regard to its crystal packing.

Since the molecular structures of **3a** and **3b** differ only with respect to their dihedral angles between the N(1)−Mg−N(2) and N(1)−C(1)−C(2)−N(2) planes, being, as expected, rather small in both cases, [6.7° (**3a**), 14.6° (**3b**)], one can suggest that the different colours of their crystals may be a result of the difference in ligand-to-metal charge transfer. Alternatively, the difference in colour may be attributed to differences in the mutual arrangement of the complex molecules and the lattice benzene molecules and thus to differences in the kind of charge transfer between them. The question as to why **3a**, **3b** and **3c** never jointly crystallise in one and the same crop and what forces determine the kind of crystal growth cannot yet be answered. The repeated crystallisation of **4** from benzene did not cause any change in the complex.

The dissolution of **1** in hot pyridine (60 to 70 °C) results in a replacement of the THF ligands by pyridine ligands and formation of (2,6-*i*$Pr_2C_6H_3$-BIAN)$Mg(py)_3\cdot(py)_2$ (**5**), which separates as black prismatic crystals on cooling the concentrated pyridine solution to ambient temperatures.

Molecular Structures of 1, 2, 3a, 3b, 4, and 5

Prior to the detailed discussion of each structure, some general remarks on the structure of the complexes should be made:

a) The 2,6-*i*$Pr_2C_6H_3$-BIAN molecule acts as a rigid, chelating ligand. Probably due to the bulkiness of the 2,6-*i*$Pr_2C_6H_3$ groups, the complexes crystallise from different solvents as monomers. The metal atoms deviate to a varying degree from the 1,2-diimonoacenaphthene plane, forming dihedral angles of 5.7° (**1**), 10.3° (**2**), 6.7° (**3a**), 14.6° (**3b**), 11.1° (**4**), and 12.3° (**5**) (Figure 1). These dihedral angles are somewhat larger than those in the magnesium DAD complexes [RN(Ph)CC(Ph)NR]$Mg(DME)_2$ (3.0°, R = Ph; 5.0°, R = *p*-MeC_6H_4), but much smaller than those in the analogous calcium complex (40.0°, R = *p*-MeC_6H_4).[18]

b) The two-electron reduction of the diimine moiety causes a reorganization of the bonds from Ar-N=C(R)-(R)C=N-Ar to $[(Ar)N\text{-}(R)C{=}C(R)\text{-}N(Ar)]^{2-}$. Thus, the dianionic nature of the 2,6-*i*$Pr_2C_6H_3$-BIAN ligand in the complexes **1** to **5** must be apparent from a shortening of the C(1)−C(2) bond and an elongation of the N(1)−C(1) and N(2)−C(2) bonds compared to the respective bond lengths in metal complexes containing the ligand in the neutral form. Actually, the C(1)−C(2) bonds in **1**−**5**, ranging from 1.389 to 1.409 Å, are shorter than those in (2,6-*i*$Pr_2C_6H_3$-BIAN)$CuCl_2$(AcOH) (1.500 Å)[7a] and [(2,6-*i*$Pr_2C_6H_3$-BIAN)$CuBr]_2$ (1.517 Å),[7b] and the N(1)−C(1) and N(2)−C(2) bonds in **1**−**5** (1.378 to 1.402 Å) are longer than those in the above $CuCl_2$ (av. 1.287 Å)[7a] and CuBr complexes (1.285 Å).[7b]

c) Another general feature of the molecular structure of complexes **1**−**5** is the fact that one of the solvent ligands fits into the pocket formed by two isopropyl groups, one of each *N*-phenyl moiety (Figure 1). The angles between the diiminoacenaphthene moiety, the metal atom, and the donor atom of the ligand located in this pocket range from 92 to 116°. A similar situation has been observed in the complex (2,6-*i*$Pr_2C_6H_3$-BIAN)$CuCl_2$(AcOH)[7a] in which the acetic acid molecule occupies the vertex of a square pyramid (O−Cu−N 95.4 and 94.6°) and two N and two Cl atoms form the square plane.

The molecular structures of **1**, **2**, **3a**, **4**, and **5** are depicted in Figures 2−6, respectively (the figure of the molecular

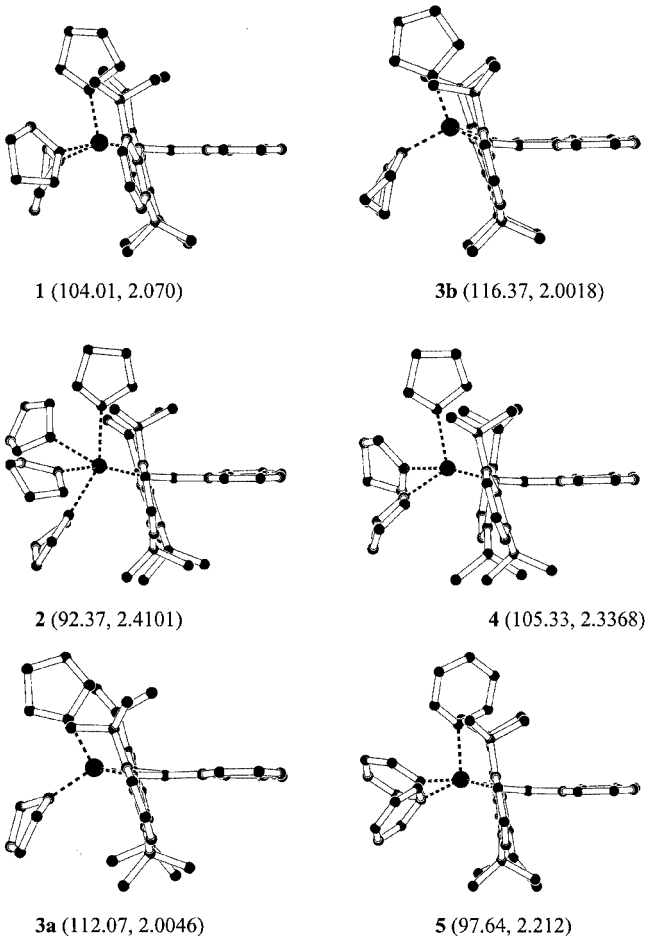

Figure 1. View of the molecules **1**−**5** along the acenaphthylene plane; the angles (deg) between the plane formed by the acenaphthene moiety, the metal, and the solvent donor atom, which is located between two isopropyl groups of the N bonded aryls, are given in parentheses along with the respective M−O(THF) and M−N(pyridine) distances (Å)

structure of **3b** is omitted since it is almost identical to that of **3a**). The crystal data collection and structure refinement data for **1**, **2**, **3a**, **3b**, **4**, and **5** are listed in Tables 1 and 2, selected bond lengths and bond angles of the molecules of these complexes are listed in Table 3 and 4. A comparison of the main bond lengths and angles in **1**−**5** is given in Figure 7.

(2,6-*i*Pr$_2$C$_6$H$_3$-BIAN)Mg(THF)$_3$ (1): Assuming that in **1** the ligand arrangement around the Mg atom is that of a square pyramid, the basal plane, made up by the atoms N(1), N(2), O(2), and O(3), is strongly distorted towards a rhombus because the Mg−O(3) bond (2.224 Å) is significantly longer than the Mg−O(1) (2.070 Å) and the Mg−O(2) bonds (2.084 Å) and the Mg−N(2) bond (2.105 Å) is longer than the Mg−N(1) bond (2.045 Å). Furthermore, the longer Mg−O(3) bond and the longer Mg−N(2) bond are in opposite positions relative to the magnesium atom. Thus, the atoms N(2) and O(3) match much better with the axial positions of a trigonal bipyramid, the equatorial plane of which is formed by the atoms N(1), O(1) and O(2) (Figure 2). The sum of the angles (359.3°) between the Mg atom and the equatorial atoms corresponds almost exactly with the ideal value of 360°, thus indicating the absence of an umbrella-like distortion of the trigonal bipyramid. Owing to the higher rigidity of the 2,6-*i*Pr$_2$C$_6$H$_3$-BIAN ligand compared to the β-diketiminate ligand, the bite angle N(1)−Mg−N(2) in **1** (84.8°) is smaller than that of the β-diketiminate ligand in (2,6-*i*PrC$_6$H$_3$NCMe)$_2$CHMg(R)(THF) (98.8° for R = O-*t*Bu, 92.8° for R = N-*i*Pr$_2$).[15e]

(2,6-*i*Pr$_2$C$_6$H$_3$-BIAN)Ca(THF)$_4$·(THF)$_{1/2}$ (2): Due to the larger ionic radius of Ca^{2+} compared to Mg^{2+} (1.00 and 0.72 Å, respectively, for six-coordinate ions[22]), the calcium atom is coordinated by four THF molecules which, along with the bidentate 2,6-*i*Pr$_2$C$_6$H$_3$-BIAN ligand, surround the calcium atom in a distorted octahedral fashion (Figure 3). One of the four Ca−O(THF) bonds is longer [Ca−O(4) 2.619 Å] than the other three which are in a fairly narrow range (2.410−2.458 Å). In contrast to the Mg−N bonds in **1**, the two Ca−N bonds (2.396 and 2.382 Å) are almost of the same length, but, as expected, longer by about 0.3 Å. The distorted octahedron is made up by O(4) and N(1) in the axial positions and O(1), O(2), O(3), and N(2) forming the equatorial plane. This distortion is caused by both the crowding around the calcium atom and the small bite angle N(1)−Ca−N(2) (75.8°), this angle being the smallest among complexes **1**−**5**.

(2,6-*i*Pr$_2$C$_6$H$_3$-BIAN)Mg(THF)$_2$·(C$_6$H$_6$)$_{1/2}$ (3a) and (2,6-*i*Pr$_2$C$_6$H$_3$-BIAN)Mg(THF)$_2$·(C$_6$H$_6$)$_2$ (3b): Despite the different crystallographic parameters, the different crystal packing and the difference in the number of the lattice solvent molecules, **3a** and **3b** exhibit almost the same molecular structure, showing a distorted tetrahedral ligand arrangement around the central Mg atom. For this reason only the structure of **3a** is depicted (Figure 4) and discussed. The two Mg−O bonds and the two Mg−N bonds do not differ markedly in length [Mg−O(1) 2.005, Mg−O(2) 1.999 Å; Mg−N(1) 1.994, Mg−N(2) 2.004 Å]. The Mg−N bonds are notably shorter than those in **1**, and, as a consequence, the bite angle N(1)−Mg−N(2) in **3a** (90.7°) is larger than in **1** (84.8°). Although the sum of the angles N(1)−Mg−N(2), N(1)−Mg−O(2) and N(2)−Mg−O(2) of 332.7° approaches the value of 328.5° for an ideal tetrahedral MgN_2O_2 moiety, a considerable distortion of the tetrahedron is apparent from the bite angle (90.7°) and the angle O(1)−Mg−O(2) (96.2°), both of which deviate significantly from the ideal value of 109.5°.

(2,6-*i*Pr$_2$C$_6$H$_3$-BIAN)Ca(THF)$_3$ (4): Except for the fact that all bonds in **4** are longer than the respective bonds in **1**, the molecular structures of **1** and **4** (Figure 5) are very similar and correspond to a trigonal bipyramid. Similar to **1**, the two Ca−N bonds differ in their length [Ca−N(1) 2.290 Å, Ca−N(2) 2.345 Å] and one of the Ca−O(THF) bonds, the Ca−O(3) bond (2.445 Å), is considerably longer than the other two, which in turn are essentially equal in length [Ca−O(1) 2.337 Å, Ca−O(2) 2.338 Å]. Thus, O(3) and N(2) are the apical atoms of the trigonal bipyramid and the equatorial plane is formed by the atoms N(1), O(1), and O(2). Also, the sum of the basal bond angles N(1)−Ca−O(1), N(1)−Ca−O(2) and O(1)−Ca−O(2)

Table 1. Crystal data and structure refinement details for **1**, **4** and **5**

Compound	(BIAN)Mg(THF)$_3$ (**1**)	(BIAN)Ca(THF)$_3$ (**4**)	(BIAN)Mg(py)$_3$ (**5**)
Empirical formula	$C_{48}H_{64}MgN_2O_3$	$C_{48}H_{64}CaN_2O_3$	$C_{51}H_{55}MgN_5{\cdot}2(C_5H_5N)$
Molecular weight	741.32	757.09	920.51
Temperature, K	173(2)	100(2)	173(2)
Crystal system	monoclinic	orthorhombic	monoclinic
Space group	*Cc* (No.9)	$P2_12_12_1$ (No.19)	$P2_1/c$ (No.14)
Unit cell dimensions	a = 22.6706(3), b = 10.8552(2) c = 18.6094(3) Å; β = 111.038(1)°	a = 11.3799(7), b = 18.6296(11) c = 20.2251(12) Å	a = 20.6168(4), b = 13.1957(3) c = 19.3918(3) Å; β = 92.416(1)°
Volume, Å^3	4274.39(12)	4287.8(4)	5270.91(18)
Z	4	4	4
Density (calculated), g/cm^3	1.152	1.173	1.160
Absorption coefficient, mm^{-1}	0.084	0.188	0.079
F(000)	1608	1640	1968
Crystal size, mm^3	0.40 × 0.38 × 0.10	0.50 × 0.50 × 0.50	0.40 × 0.38 × 0.28
θ range for data collection, deg	1.92 to 25.00	2.01 to 24.00	0.99 to 25.00
Index ranges	$-22 \le h \le 26$, $-12 \le k \le 12$, $-22 \le l \le 22$	$-13 \le h \le 13$, $-21 \le k \le 21$, $-23 \le l \le 23$	$-16 \le h \le 24$, $-15 \le k \le 15$, $-16 \le l \le 23$
Reflections collected	10447	29339	14996
Independent reflections	4982 [R(int) = 0.0999]	6695 [R(int) = 0.0320]	9004 [R(int) = 0.1138]
Max/min transmission	0.9924/0.7456	0.9117/0.9117	0.9655/0.5598
Data/restraints/parameters	4982/2/505	6695/38/647	9004/0/630
Goodness-of-fit on F^2	1.000	1.136	1.033
Final R indices [$I > 2\sigma(I)$]	$R1$ = 0.0641, $wR2$ = 0.1151	$R1$ = 0.0432, $wR2$ = 0.1078	$R1$ = 0.0798, $wR2$ = 0.1474
R indices (all data)	$R1$ = 0.1214, $wR2$ = 0.1356	$R1$ = 0.0464, $wR2$ = 0.1094	$R1$ = 0.2300, $wR2$ = 0.1923
Absolute structure parameter	−0.5(5)	0.03(3)	−
Largest diff. peak and hole, e/Å^3	0.242 and −0.273	0.394 and −0.185	0.291 and −0.295

Table 2. Crystal data and structure refinement details for **2**, **3a** and **3b**

Compound	(BIAN)Ca(THF)$_4$ (**2**)	(BIAN)Mg(THF)$_2$ (**3a**)	(BIAN)Mg(THF)$_2$ (**3b**)
Empirical formula	$C_{52}H_{72}CaN_2O_4{\cdot}1/2(C_4H_8O)$	$C_{44}H_{56}MgN_2O_2{\cdot}1/2(C_6H_6)$	$C_{44}H_{56}MgN_2O_2{\cdot}2(C_6H_6)$
Molecular weight	865.25	708.27	825.43
Temperature, K	173(2)	100(2)	100(2)
Crystal system	monoclinic	monoclinic	orthorhombic
Space group	$P2_1/n$ (No.14)	$P2_1/n$ (No.14)	*Pbca* (No.61)
Unit cell dimensions	a = 13.3251(1), b = 18.7219(3) c = 19.9719(3) Å; β = 99.857(1)°	a = 11.8702(7), b = 16.7665(10) c = 20.7019(12) Å; β = 96.0960(10)°	a = 18.7994(13), b = 21.1341(15) c = 24.4612(17) Å
Volume, Å^3	4908.86(11)	4096.8(4)	9718.6(12)
Z	4	4	8
Density (calculated), g/cm^3	1.171	1.148	1.128
Absorption coefficient, mm^{-1}	0.175	0.083	0.079
F(000)	1880	1532	3568
Crystal size, mm^3	0.56 × 0.24 × 0.20	0.10 × 0.10 × 0.10	0.40 × 0.40 × 0.20
θ range for data collection, deg	1.50 to 27.50	1.90 to 29.02	1.66 to 23.30
Index ranges	$-17 \le h \le 17$, $-24 \le k \le 18$, $-25 \le l \le 25$	$-10 \le h \le 16$, $-22 \le k \le 22$, $-28 \le l \le 26$	$-20 \le h \le 20$, $-23 \le k \le 23$, $-27 \le l \le 27$
Reflections collected	36143	29759	62079
Independent reflections	11270 [R(int) = 0.0875]	10865 [R(int) = 0.0191]	6997 [R(int) = 0.0409]
Max/min transmission	0.9766/0.6809	0.9918/0.9918	0.9844/0.9692
Data/restraints/parameters	11270/4/578	10865/0/705	6997/6/809
Goodness-of-fit on F^2	1.010	1.027	1.040
Final R indices [$I > 2\sigma(I)$]	$R1$ = 0.0646, $wR2$ = 0.1357	$R1$ = 0.0425, $wR2$ = 0.1066	$R1$ = 0.0377, $wR2$ = 0.0984
R indices (all data)	$R1$ = 0.1265, $wR2$ = 0.1624	$R1$ = 0.0548, $wR2$ = 0.1158	$R1$ = 0.0499, $wR2$ = 0.1109
Absolute structure parameter	−	−	−
Largest diff. peak and hole, e/Å^3	0.425 and −0.453	0.448 and −0.187	0.274 and −0.196

(359.8°) coincides with that of **1** (359.3°) and corresponds with the ideal value of 360°. Because of the longer Ca−N bonds compared to the Mg−N bonds in **1**, the bite angle N(1)−M−N(2) in **4** (M = Ca; 77.0°) is smaller than in **1** (M = Mg; 84.8°). A closer look at the structures of **1** and **4** establishes that the molecules are enantiomorphic (see

Table 3. Selected bond lengths (Å) and angles (deg) for Mg complexes **1**, **3a**, **3b** and **5**

	1	3a	3b	5
Mg−N(1)	2.045(5)	1.9945(9)	1.9937(11)	2.103(4)
Mg−N(2)	2.105(5)	2.0038(9)	1.9951(12)	2.071(4)
Mg−C(1)	2.811(6)	2.6778(11)	2.6515(13)	2.828(5)
Mg−C(2)	2.817(6)	2.6900(11)	2.6520(14)	2.805(5)
Mg−L(1)[a]	2.070(4)	2.0046(9)	2.0018(10)	2.198(5)
Mg−L(2)	2.084(4)	1.9994(8)	2.0001(10)	2.212(5)
Mg−L(3)	2.224(4)			2.271(5)
N(1)−C(1)	1.401(6)	1.3965(13)	1.3933(17)	1.400(6)
N(1)−C(13)	1.408(7)	1.4166(12)	1.4192(17)	1.431(6)
N(2)−C(2)	1.378(7)	1.3893(13)	1.3945(17)	1.386(6)
N(2)−C(25)	1.419(7)	1.4170(12)	1.4125(17)	1.422(6)
C(1)−C(2)	1.389(7)	1.3976(13)	1.3916(18)	1.392(6)
N(1)−Mg−N(2)	84.77(18)	90.71(4)	91.12(5)	84.94(17)
N(1)−Mg−L(1)	105.83(18)	115.30(4)	118.72(5)	91.47(17)
N(1)−Mg−L(2)	154.17(18)	117.74(4)	117.78(5)	95.44(18)
N(1)−Mg−L(3)	90.42(17)			168.27(19)
N(2)−Mg−L(1)	102.14(18)	114.19(4)	115.61(5)	149.89(18)
N(2)−Mg−L(2)	95.95(19)	124.32(4)	115.45(5)	106.43(18)
N(2)−Mg−L(3)	164.16(18)			95.24(18)
L(1)−Mg−L(2)	99.28(17)	96.24(4)	99.45(4)	103.67(18)
L(1)−Mg−L(3)	93.69(16)			82.48(17)
L(2)−Mg−L(3)	81.89(17)			95.75(17)
C(1)−N(1)−Mg	107.9(3)	102.89(6)	101.57(8)	105.9(3)
C(13)−N(1)−Mg	130.2(3)	139.01(7)	140.86(9)	137.8(3)
C(2)−N(2)−Mg	106.0(3)	103.40(6)	101.49(8)	106.8(3)
C(25)−N(2)−Mg	134.2(4)	138.08(7)	139.82(9)	134.3(3)

[a] For **1** and **5** L(1), L(2), L(3) are O(1), O(2), O(3) and N(3), N(4), N(5), respectively; for **3a** and **3b** L(1) and L(2) are O(1) and O(2).

Figure 7). One can suggest that in solutions of the compounds, the structures may interconvert by splitting off and recoordinating a THF ligand, thus forming four-coordinate species B and B′ as intermediates (Scheme 2). We propose such a process in order to explain the broadened aryl signals in the ^{1}H NMR spectrum of **1** (see below).

(2,6-*i*Pr$_2$C$_6$H$_3$-BIAN)Mg(py)$_3$·(py)$_2$ (5): The structure of complex **5** (Figure 6) corresponds with the trigonal-bipyramidal structures of the five-coordinate complexes **1** and **4** except that the axial and equatorial positions in **5** are not as pronounced as in **1** and **4**. The axial positions of N(1) and N(5) are apparent from the angle N(1)−Mg−N(5) of 168.3°, but the distances of N(1) and N(5) to the magnesium atom [Mg−N(1) 2.103 Å, Mg−N(5) 2.271 Å] do not differ all that much from those of the other three N−Mg distances [Mg−N(2) 2.071, Mg−N(3) 2.198 Å, Mg−N(4) 2.212 Å]. The sum of the bond angles between the Mg atom and N(2), N(3), and N(4) is exactly 360°, thus indicating that the Mg atom lies perfectly in the equatorial plane of the bipyramid. The bite angle N(1)−Mg−N(2) (84.9°) can be considered to be equal to that in complex **1** (84.8°). A closer inspection of the crystal structure of **5** shows that one of the CH_3 groups of the 2,6-*i*Pr$_2$C$_6$H$_3$-BIAN ligand is turned towards the magnesium atom, but keeps away from the metal by ≥ 3 Å (Figure 8). In the case of complex **1** this contact is less evident due to the overcrowding around the magnesium atom arising from the shorter Mg−O distances and the non-flat shape of the THF ligands.

Table 4. Selected Bond lengths (Å) and Angles (deg) for Ca complexes **2** and **4**

	2	4
Ca−N(1)	2.396(2)	2.2901(18)
Ca−N(2)	2.382(2)	2.3454(18)
Ca−C(1)	3.118(2)	3.041(2)
Ca−C(2)	3.123(2)	3.056(2)
Ca−O(1)	2.4101(18)	2.3368(16)
Ca−O(2)	2.439(2)	2.3380(17)
Ca−O(3)	2.4578(19)	2.4449(17)
Ca−O(4)	2.6187(18)	
N(1)−C(1)	1.391(3)	1.384(3)
N(1)−C(13)	1.423(3)	1.407(3)
N(2)−C(2)	1.402(3)	1.384(3)
N(2)−C(25)	1.418(3)	1.405(3)
C(1)−C(2)	1.409(3)	1.397(3)
N(1)−Ca−N(2)	75.76(7)	77.04(6)
N(1)−Ca−O(1)	91.27(7)	115.23(6)
N(1)−Ca−O(2)	91.11(7)	140.12(7)
N(1)−Ca−O(3)	117.68(7)	93.31(6)
N(1)−Ca−O(4)	163.44(7)	
N(2)−Ca−O(1)	106.00(7)	102.12(6)
N(2)−Ca−O(2)	160.10(7)	98.00(7)
N(2)−Ca−O(3)	90.66(7)	166.24(6)
N(2)−Ca−O(4)	111.68(7)	
O(1)−Ca−O(2)	88.91(7)	104.55(7)
O(1)−Ca−O(3)	149.70(7)	90.82(6)
O(1)−Ca−O(4)	72.60(6)	
O(2)−Ca−O(3)	82.17(7)	83.03(6)
O(2)−Ca−O(4)	85.02(7)	
O(3)−Ca−O(4)	77.80(6)	
C(1)−N(1)−Ca	107.85(14)	109.19(13)
C(13)−N(1)−Ca	135.38(16)	129.79(13)
C(2)−N(2)−Ca	108.47(14)	107.20(13)
C(25)−N(2)−Ca	133.24(16)	133.49(14)

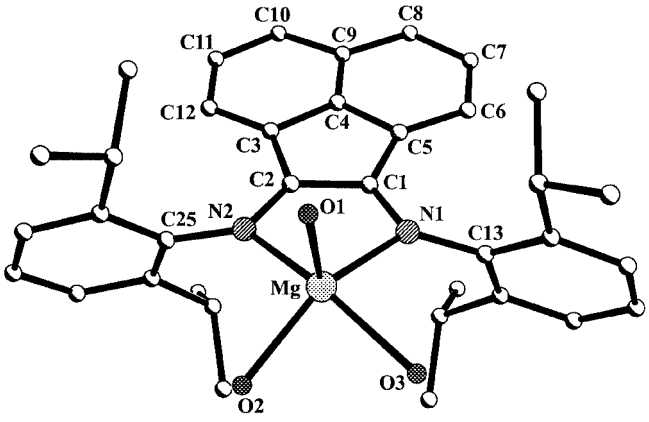

Figure 2. PLATON plot[21] of the molecular structure and the numbering scheme of **1**; all hydrogens and the carbon atoms of the THF ligands have been omitted

NMR Studies on Solutions of 1 and 5: The solution behaviour of the five-coordinate complexes **1** in [D$_8$]THF and **5** in [D$_5$]pyridine is rather different. The broadening of the aromatic signals in the ^{1}H NMR spectrum of **1** (see Figure 9a) can be explained by a dynamic process in the metal coordination sphere connected with a change in the coordination number of the magnesium atom from five to four (Scheme 2). Similar processes have been observed for THF

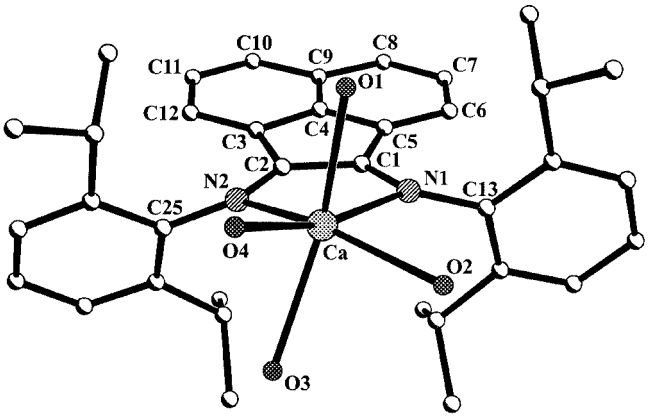

Figure 3. PLATON plot[21] of the molecular structure and the numbering scheme of **2**; all hydrogens and the carbon atoms of the THF ligands have been omitted

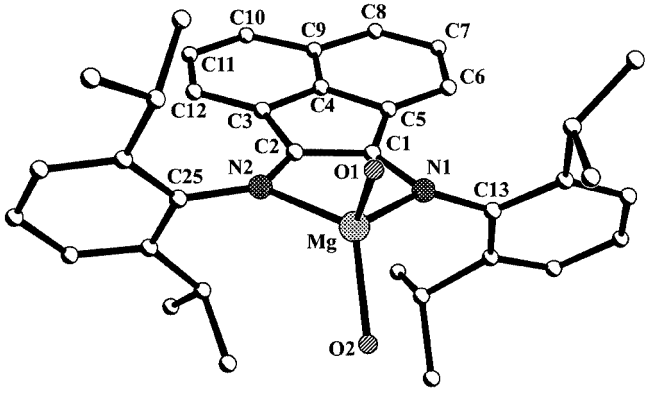

Figure 4. PLATON plot[21] of the molecular structure and the numbering scheme of **3a**; all hydrogens and the carbon atoms of the THF ligands have been omitted

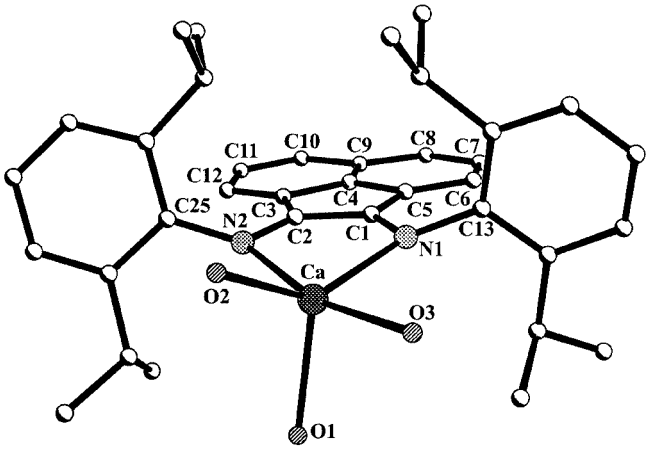

Figure 5. PLATON plot[21] of the molecular structure and the numbering scheme of **4**; all hydrogens and the carbon atoms of the THF ligands have been omitted

solutions of the β-diketiminato complexes (2,6-iPrC$_6$H$_3$NCMe)$_2$CHMgR (R = N-iPr$_2$, O-tBu).[15e] The change in the coordination number of the magnesium effects the electronic properties of the planar diiminoacenaphthene system and explains the broadening of its proton

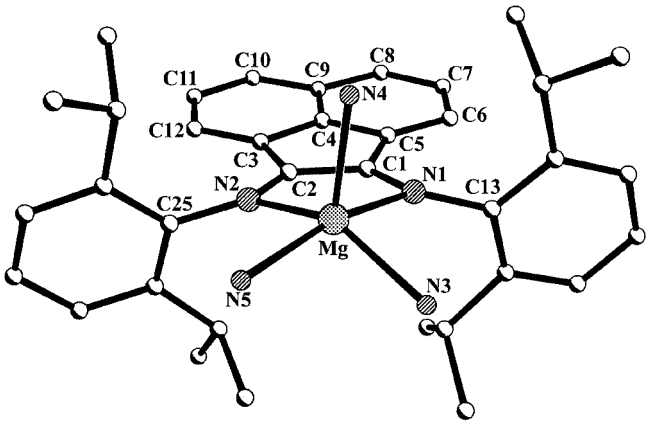

Figure 6. PLATON plot[21] of the molecular structure and the numbering scheme of **5**; all hydrogens and the carbon atoms of the py ligands have been omitted

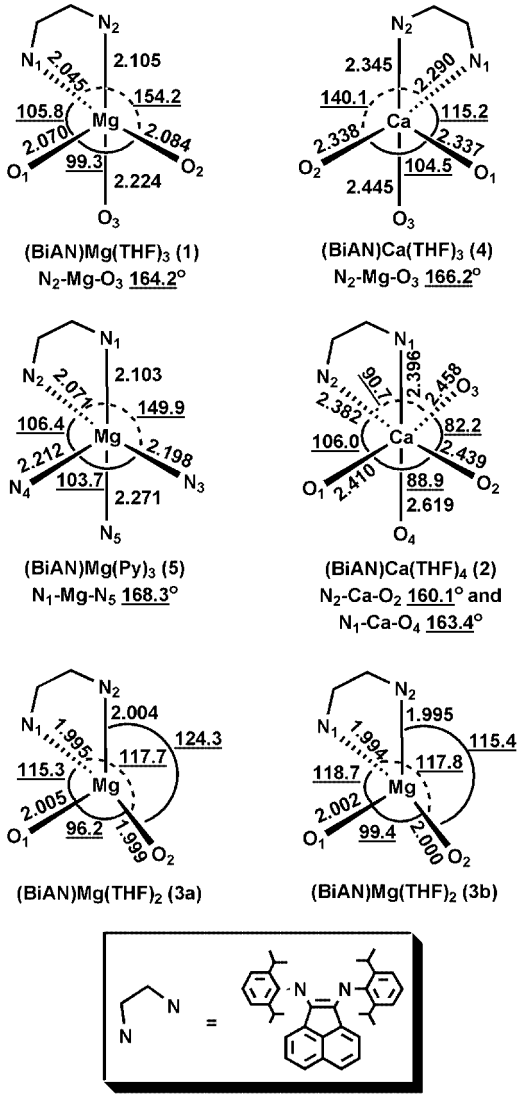

Figure 7. Comparison of the main bond lengths (Å) and angles (deg) in **1**–**5**

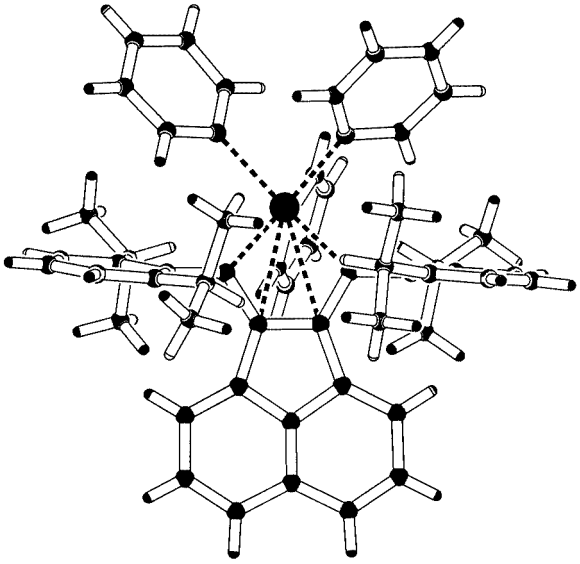

Figure 8. View of **5**, emphasising the tendency of one CH_3 group to interact with the Mg atom

signals. Since the 2,6-*i*$Pr_2C_6H_3$ groups are attached in an almost orthogonal fashion to the five-membered metallacycle C_2N_2Mg [due to the restricted rotation around the C(*ipso*)−N bond] the electronic changes at the metal do not influence the 2,6-*i*$Pr_2C_6H_3$ groups substantially, thus causing a normal shape of the isopropyl methyl and the isopropyl methine signals (two doublets and a septet, respectively). On going from THF to benzene as the solvent, the NMR spectrum of **1** does not change significantly. At this point it should be noted that the ^{1}H NMR spectrum of (2,6-*i*PrC_6H_3-BIAN)$Mg(THF)_2\cdot(C_6H_6)_{1/2}$ (**3a**) (Figure 9b), containing four-coordinate magnesium, does not indicate the formation of a three-coordinate species by splitting off of one of the two THF ligands.

The ^{1}H NMR spectrum of **5** in [D_5]pyridine (Figure 9c) exhibits four isopropyl methyl signals of different intensity at δ = 1.26 (bs), 1.19 (d), 1.13 (d), and 0.86 ppm (bs), two of which are significantly broadened. The isopropyl methine proton signal centred at δ = 3.84 ppm (spt) corresponds to the two methyl doublets at δ = 1.19 and 1.13 ppm, whereas the chemical shift of the methine proton signal corresponding to the two broadened isopropyl methyl signals is

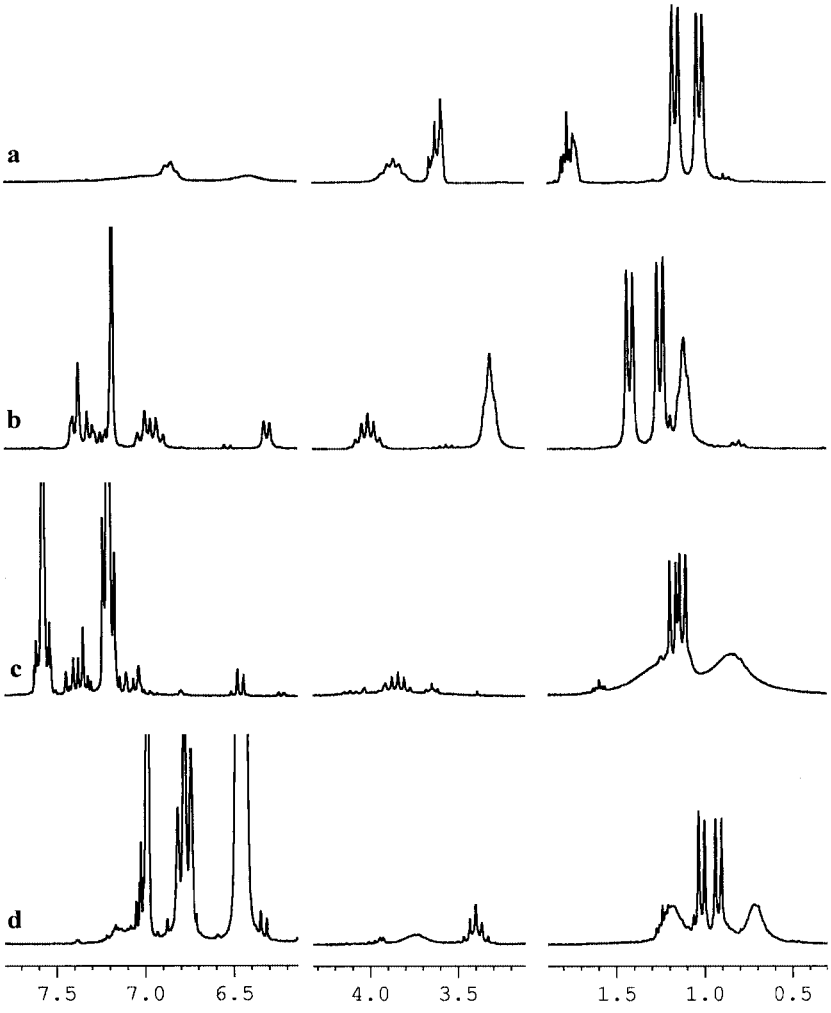

Figure 9. ^{1}H NMR spectra (200 MHz) of **1** in [D_8]THF (a) and C_6D_6 (b) and of **5** in [D_5]pyridine (c) and C_6D_6 (d)

impossible to ascertain because of its extreme broadening. However, in the ^{1}H NMR spectrum of **5** in C_6D_6 (Figure 9d), the two methine proton signals corresponding to the four isopropyl methyl proton signals at δ = 1.38 (bs), 1.21 (d), 1.12 (d), and 0.91 ppm (bs) can be located at δ = 3.93 (bs) and 3.59 ppm (spt). In this case, the four methyl signals are approximately of equal intensity, whereas in the spectrum of **5** recorded in pyridine (Figure 9c), the broadened methyl signals are more intense. For comparison, in the ^{1}H NMR spectrum of the free 2,6-*i*Pr$_2$C$_6$H$_3$-BIAN ligand in [D$_5$]pyridine three signals represent the isopropyl protons, two doublets at δ = 1.27 (12 H) and 1.07 ppm (12 H) for the methyl protons and a septet at δ = 3.24 ppm (4 H) for the methine protons. The difference in the integrals of the four methyl signals in the spectra of **5** in [D$_5$]pyridine and in C_6D_6 evidently indicates the presence of two different species in both solutions. When using pyridine as the solvent for **5**, the removal of one of the three pyridine ligands from the magnesium atom, and thus the formation of a four-coordinate species, as discussed in the case of complex **1** for a THF ligand (see Scheme 2), should be considerably suppressed. Furthermore, the Mg−N(py) bonds are stronger than the Mg−O(THF) bonds due to the higher donor strength of pyridine compared to THF (33.1 and 20.0, correspondingly vs. $SbCl_5$).[23] Therefore, we suggest that besides the dynamic dissociation-recoordination process connected with a change in the coordination number of the magnesium atom, a second process (slow on the NMR time scale) will take place in solutions of **5** in pyridine, as well as in benzene, consisting of a distortion of the coordination sphere of the metal without a change of its coordination number. In the case of **5**, the well-known Berry pseudorotation[24,25] of five-coordinate complexes cannot serve as an explanation because of the constraints imposed by the chelating ring system and the molecular structure of **5**, which is best described as a distorted trigonal bipyramid and not as a square pyramid. We therefore suppose that in solutions of **5**, a distortion of the trigonal bipyramid occurs, in the course of which the nitrogen atoms N(1) and N(2) change their positions from axial to equatorial and vice versa (Scheme 3). A weak interaction between the Mg atom and the CH_3 groups may play some role in this process.

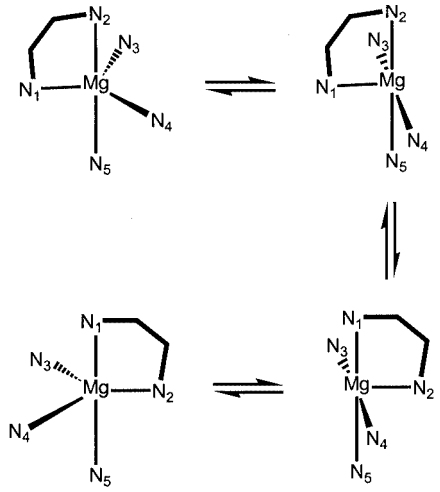

Scheme 3

Conclusion

We have synthesised and characterised magnesium and calcium complexes with the dianionic 1,2-bis[(2,6-diisopropylphenyl)imino]acenaphthene ligand. The sterically demanding substituents at both nitrogen atoms cause the formation of monomeric species. In the near future, we intend to investigate the reactivity of these complexes towards different organic substrates, such as ketones, organic halides and unsaturated organic compounds in order to find out whether these magnesium and calcium complexes may serve as one- and two-electron reductants. Preliminary studies have shown that the reactions of complex **1** with $Ph_2C{=}O$ or Me_3SiCl afford a pinacone coupling product or a product formed by the two-electron oxidative addition of Me_3SiCl to the complex, respectively.

Experimental Section

General Remarks: All manipulations were carried out under vacuum in Schlenk tubes. Tetrahydrofuran and benzene were distilled from sodium/benzophenone. Pyridine was distilled and further treated with small amounts of sodium and then condensed in vacuo immediately prior to use. The deuterated solvents [D$_8$]THF, C_6D_6, and [D$_5$]pyridine (Aldrich) were dried at ambient temperature over sodium/benzophenone (THF, benzene) or sodium (pyridine) and, just prior to use, condensed under vacuum into the NMR tubes containing the compounds. Melting points were measured in sealed capillaries. 1,2-Bis[(2,6-diisopropylphenyl)imino]acenaphthene (2,6-*i*Pr$_2$C$_6$H$_3$-BIAN) was prepared according to the published procedure.[7a] The excess of Mg and Ca left after the preparation of **1** and **2** was used without further activation by CH_2I_2 for the repeated synthesis of these complexes. The IR spectra were recorded on a Specord M80 spectrometer and the UV/Vis spectra on a Specord M80. The ^{1}H and ^{13}C{^{1}H} NMR spectra were recorded on a Bruker DPX-200 NMR spectrometer (^{1}H, 200 MHz; ^{13}C, 50.32 MHz). Chemical shifts are reported in ppm relative to the ^{1}H and ^{13}C{^{1}H}- residues of the deuterated solvents.

(2,6-*i*Pr$_2$C$_6$H$_3$-BIAN)Mg(THF)$_3$ (1): Magnesium shavings (2.4 g, 100 mmol) and CH_2I_2 (0.8 g, 2.98 mmol) were placed in a Schlenk-like ampoule (ca. 100 mL volume) equipped with a Teflon stopcock. After evacuation of the ampoule (10^{-1} Torr within ca. 1 min), THF (40 mL) was added by condensation and the mixture was stirred for 2 h. The $MgI_2(THF)_n$ formed was decanted together with the solvent and the residual metal was washed three times with THF (40 mL). A suspension of 2,6-*i*Pr$_2$C$_6$H$_3$-BIAN (0.5 g, 1.0 mmol) in THF (30 mL) was then added to the activated magnesium metal and the mixture was refluxed. In the course of about 10 min reflux, the reaction mixture turned deep green. The solution was then cooled to ambient temperature and decanted from the excess of magnesium. Crude **1** (0.69 g, 93%) was obtained as a deep-red crystalline solid on removal of the volatiles from the solution in vacuo. Recrystallisation of **1** from THF (15 mL) yielded large block-like crystals (0.27 g, 37%) and further **1** (0.31 g, 42%)

was obtained by concentration of the mother liquor. M.p. 176 °C (decomp.). ^{1}H NMR ([D$_8$]THF, 20 °C): δ = 8.0−4.5 (br. m, 12 H, C$_{arom}$), 3.85 (spt, 4 H, C*H*Me$_2$), 3.61 [m, 8 H, α-C*H*$_2$(THF)], 3.58 [s, 8 H, α-C*H*$_2$(THF)], 1.76 [m, 4 H, β-C*H*$_2$(THF)], 1.73 [s, 4 H, β-C*H*$_2$(THF)], 1.16 [d, ^3J = 8.0 Hz, 12 H, CH(C*H*$_3$)$_2$], 1.03 [d, ^3J = 6.0 Hz, 12 H, CH(C*H*$_3$)$_2$]. IR (Nujol): $\tilde{\nu}$ = 1580 s, 1410 s, 1315 vs, 1250 s, 1170 m, 1105 w, 1020 s, 910 m, 875 s, 800 m, 760 vs, 615 m cm^{-1}. UV/Vis (THF, 20 °C): λ_{max} = 822, 370 nm. $C_{48}H_{64}MgN_2O_3$ (741.32): calcd. C 77.77, H 8.70, Mg 3.28; found C 77.02, H 8.13, Mg 3.26.

(2,6-*i*Pr$_2$C$_6$H$_3$-BIAN)Ca(THF)$_4$·(THF)$_{1/2}$ (2): Calcium metal granules (5.5 g, 137 mmol) were activated by CH_2I_2 (0.8 g, 2.98 mmol) as described for **1**. The activated Ca was treated with 2,6-*i*Pr$_2$C$_6$H$_3$-BIAN (0.5 g, 1.0 mmol) in THF (30 mL) and the mixture was stirred under reflux for 1 h. After cooling the mixture to ambient temperature, the solution was decanted from the excess of Ca metal. Evaporation of the solvent in vacuo afforded 0.75 g (85%) of crude **2** as deep-red crystals. Analytically pure, black coloured **2** was isolated by concentration of the decanted solution under reflux to 15 mL and cooling of the concentrate to ambient temperature. M.p. >160 °C (decomp.). ^{1}H NMR ([D$_8$]THF, 20 °C): δ = 8.0−5.0 (br. m, 12 H, C$_{arom}$), 3.9 (br. m, 4 H, C*H*Me$_2$), 3.63 (m, 8 H, α-C*H*$_2$(THF)], 3.60 [s, 8 H, α-C*H*$_2$(THF)], 1.78 [m, 8 H, β-C*H*$_2$(THF)], 1.75 [s, 8 H, β-C*H*$_2$(THF)], 1.18 [s, 24 H, CH(C*H*$_3$)$_2$]. IR (Nujol): $\tilde{\nu}$ = 1585 s, 1405 s, 1310 vs, 1250 s, 1170 m, 1100 w, 1020 m, 1010 m, 910 m, 870 s, 800 m, 760 vs, 620 m cm^{-1}. $C_{52}H_{72}CaN_2O_4(C_4H_8O)_{1/2}$ (865.25): calcd. C 74.96, H 8.85, Ca 4.63; found C 74.13, H 8.47, Ca 4.41.

(2,6-*i*Pr$_2$C$_6$H$_3$-BIAN)Mg(THF)$_2$·(C$_6$H$_6$)$_{1/2}$ (3a): Complex **1** (0.69 g, 0.93 mmol) dried in vacuo for 1 h, was dissolved in benzene (20 mL) and the solution was heated to 70−80 °C. The volume of the green benzene solution was than reduced to 10 mL by evaporation in vacuo at 70 °C. After cooling the solution to ambient temperature khaki-green crystals of **3a** (0.31 g, 47%) separated within 24 h. M.p. > 260 °C. ^{1}H NMR (C$_6$D$_6$, 20 °C): δ = 7.38−7.20 (m, 6 H, C$_{arom}$), 7.02−6.87 (m, 4 H, C$_{arom}$), 6.29 (d, ^3J = 8.0 Hz, 2 H), 3.99 (spt, 4 H, C*H*Me$_2$), 3.30 [s, 8 H, α-C*H*$_2$(THF)], 1.41 [d, ^3J = 6.0 Hz, 12 H, CH(C*H*$_3$)$_2$], 1.23 [d, 12 H, ^3J = 6.0 Hz, CH(C*H*$_3$)$_2$], 1.08 [s, 4 H, β-C*H*$_2$(THF)]. IR (Nujol): $\tilde{\nu}$ = 1605 w, 1575 s, 1415 vs, 1300 vs, 1250 s, 1170 m, 1100 w, 1020 s, 910 m, 905 s, 870 s, 800 m, 760 vs, 680 s, 615 m cm^{-1}. UV/Vis (C$_6$H$_6$, 20 °C): λ_{max} = 750, 370 nm. $C_{44}H_{56}MgN_2O_2(C_6H_6)_{1/2}$ (708.27): calcd. C 79.70, H 8.40, Mg 3.43; found C 78.61, H 7.48, Mg 3.29.

(2,6-*i*Pr$_2$C$_6$H$_3$-BIAN)Mg(THF)$_2$·(C$_6$H$_6$)$_2$ (3b): Complex **1** (0.65 g, 0.87 mmol) was heated in vacuo to 80 °C for 10 min. The solid was then dissolved in hot benzene (20 mL) and after its dissolution the solvent was evaporated in vacuo. The remaining solid was redissolved in hot benzene (20 mL), followed by evaporation of the solvent. The residue was crystallised from benzene (10 mL) at ambient temperature affording 0.25 g (34%) of **3b** as thin emerald-green crystals. M.p. ca. 180 °C (decomp.). ^{1}H NMR (C$_6$D$_6$, 20 °C): δ = 7.38−7.20 (m, 6 H, C$_{arom}$), 7.02−6.87 (m, 4 H, C$_{arom}$), 6.29 (d, ^3J = 8.0 Hz, 2 H), 3.99 (spt, 4 H, C*H*Me$_2$), 3.30 [s, 8 H, α-C*H*$_2$(THF)], 1.41 [d, ^3J = 6.0 Hz, 12 H, CH(C*H*$_3$)$_2$], 1.23 [d, ^3J = 6.0 Hz, 12 H, CH(C*H*$_3$)$_2$], 1.08 [s, 4 H, β-C*H*$_2$(THF)] ppm. IR (Nujol): $\tilde{\nu}$ = 1580 s, 1415 vs, 1300 vs, 1250 s, 1170 m, 1100 w, 1020 s, 910 m, 905 s, 870 s, 800 m, 760 vs, 680 vs, 615 m cm^{-1}. UV/Vis (C$_6$H$_6$, 20 °C): λ_{max} = 750, 370 nm. $C_{44}H_{56}MgN_2O_2(C_6H_6)_2$ (825.43): calcd. C 81.48, H 8.30, Mg 2.94; found C 81.67, H 7.88, Mg 2.62.

(2,6-*i*Pr$_2$C$_6$H$_3$-BIAN)Ca(THF)$_3$ (4): Crude **2** (0.7 g, 0.81 mmol) was dried in vacuo at ambient temperature for 10 min and was then dissolved in hot benzene (15 mL; 60−80 °C). Cooling the benzene solution to ambient temperature caused the precipitation of **4** as deep red-brown crystals within 36 h (0.38 g, 63%). M.p. 178 °C (decomp.). ^{1}H NMR (C$_6$D$_6$, 20 °C): δ = 7.38−7.21 (m, 6 H, C$_{arom}$), 6.99−6.88 (m, 4 H, C$_{arom}$), 6.35 (d, ^3J = 6.0 Hz, 2 H), 3.98 (spt, 4 H, C*H*Me$_2$), 3.39 [s, 12 H, α-C*H*$_2$(THF)], 1.41 [d, ^3J = 6.4 Hz, 12 H, CH(C*H*$_3$)$_2$], 1.32 [d, ^3J = 6.6 Hz, 12 H, CH(C*H*$_3$)$_2$], 1.17 [s, 4 H, β-C*H*$_2$(THF)]. IR (Nujol): $\tilde{\nu}$ = 1580 s, 1550 w, 1400 vs, 1320 vs, 1220 s, 1170 m, 1100 w, 1020 s, 910 s, 870 s, 850 s, 800 s, 755 vs, 680 w, 610 m cm^{-1}. $C_{48}H_{64}CaN_2O_3$ (757.09): calcd. C 76.15, H 8.52, Ca 5.29; found C 75.94, H 8.13, Ca 4.89.

(2,6-*i*Pr$_2$C$_6$H$_3$-BIAN)Mg(py)$_3$·(py)$_2$ (5): Crude **1** (0.65 g, 0.87 mmol) was dissolved in pyridine (30 mL) and the solution was heated to 60 °C. The brown solution formed was concentrated to 10 mL by evaporation of the solvent in vacuo. After one day, black crystals of **5** (0.56 g, 69%) had precipitated. M.p. 171 °C (decomp). ^{1}H NMR (C$_6$D$_6$, 20 °C): δ = 3.93 [s, 4 H, C*H*(CH$_3$)$_2$], 3.59 [spt, ^3J = 6.0 Hz, 4 H, C*H*(CH$_3$)$_2$], 1.38 [br. s, 12 H, CH(C*H*$_3$)$_2$], 1.21 [d, ^3J = 6.6 Hz, 12 H, CH(C*H*$_3$)$_2$], 1.12 [d, ^3J = 6.8 Hz, 12 H, CH(C*H*$_3$)$_2$], 0.91 [br. s, 12 H, CH(C*H*$_3$)$_2$] ppm; the signals of the aromatic protons are broadened and covered by the pyridine resonances. IR (Nujol): $\tilde{\nu}$ = 1600 m, 1580 vs, 1485 m, 1310 vs, 1250 s, 1210 m, 1170 s, 1100 w, 1070 m, 1040 m, 990 w, 910 s, 890 w, 800 m, 750 vs, 705 vs cm^{-1}. $C_{51}H_{55}MgN_5(C_5H_5N)_2$ (920.51): calcd. C 79.59, H 7.12, Mg 2.64; found C 78.94, H 6.82, Mg 2.63.

Single-Crystal X-ray Structure Determination of 1−5: The crystal data and details of data collection are given in Table 1 and 2. The data for **1**, **2**, **5**, and **3a**, **3b**, **4** were collected on a SMART CCD and a SMART APEX diffractometer, respectively (graphite-monochromated Mo-K_α radiation, ω- and ψ-scan technique, λ= 0.71073 Å). The structures were solved by direct methods using SHELXS-97[26] and were refined on F^2 using all reflections with SHELXL-97.[27] All non-hydrogen atoms were refined anisotropically and the hydrogen atoms were placed in calculated positions and assigned to an isotropic displacement parameter of 0.08 Å^2. Absolute structure parameters were determined according to the method of Flack[28] with SHELXL-97.[27] For **1**, the determination of the correct absolute structure was not possible. SADABS[29] was used to perform area-detector scaling and absorption corrections. The geometrical aspects of the structures were analysed with the PLATON program.[21]

CCDC-206142 (**1**) -206143 (**2**) -206144 (**3a**) -206145 (**3b**) -206146 (**4**) and -206147 (**5**) contain the supplementary crystallographic data for this paper. These data can be obtained free of charge at www.ccdc.cam.ac.uk/conts/retrieving.html or from the Cambridge Crystallographic Data Centre, 12, Union Road, Cambridge CB2 1EZ, UK; Fax: (internat.) +44-1223/336-033; E-mail: deposit@ccdc.cam.ac.uk.

Acknowledgments

This work was supported by the Russian Foundation for Basic Research (Grant No. 03-03-32246a), the Alexander von Humboldt Stiftung (ILF), the Fonds der Chemischen Industrie, and the Deutsche Forschungsgemeinschaft.

[1] [1a] I. Matei, T. Lixandru, *Bull. Inst. Politeh. Iasi* **1967**, *13*, 245−255. [1b] G. Manecke, J. Gauger, *Chem. Ber.* **1968**, *101*, 3326−3328. [1c] I. Matei, T. Lixandru, *Bull. Inst. Politeh. Iasi* **1969**, *15*, 57−66.

[2] [2a] R. van Asselt, E. E. C. G. Gielens, R. E. Rulke, C. J. Elsevier, *J. Chem. Soc., Chem. Commun.* **1993**, 1203−1205. [2b] R.

van Asselt, K. Vrieze, C. J. Elsevier, *J. Organomet. Chem.* **1994**, *480*, 27−40. [2c] R. van Asselt, C. J. Elsevier, W. J. J. Smeets, A. L. Spek, R. Benedix, *Recl. Trav. Chim. Pays-Bas* **1994**, *113*, 88−98. [2d] R. van Asselt, C. J. Elsevier, *Organometallics* **1994**, *13*, 1972−1980. [2e] R. van Asselt, C. J. Elsevier, W. J. J. Smeets, A. L. Spek, *Inorg. Chem.* **1994**, *33*, 1521−1531. [2f] R. van Asselt, E. Rijnberg, C. J. Elsevier, *Organometallics* **1994**, *13*, 706−720. [2g] R. van Asselt, E. E. C. G. Gielens, R. E. Rulke, K. Vrieze, C. J. Elsevier, *J. Am. Chem. Soc.* **1994**, *116*, 977−985.

[3] M. W. van Laren, C. J. Elsevier, *Angew. Chem.* **1999**, *111*, 3926−3929; *Angew. Chem. Int. Ed.* **1999**, *38*, 3715−3717.

[4] R. van Belzen, H. Hoffmann, C. J. Elsevier, *Angew. Chem.* **1997**, *109*, 1833−1835; *Angew. Chem. Int. Ed. Engl.* **1997**, *36*, 1743−1745.

[5] E. Shirakawa, T. Hiyama, *J. Organomet. Chem.* **2002**, *653*, 114−121.

[6] [6a] D. Pappalardo, M. Mazzeo, S. Antinucci, C. Pellecchia, *Macromolecules* **2000**, *33*, 9483−9487. [6b] D. J. Tempel, L. K. Johnson, R. L. Huff, P. S. White, M. Brookhart, *J. Am. Chem. Soc.* **2000**, *122*, 6686−6700. [6c] D. P. Gates, S. A. Svejda, E. Onate, Ch. M. Killian, L. K. Johnson, P. S. White, M. Brookhart, *Macromolecules* **2000**, *33*, 2320−2334. [6d] S. A. Svejda, M. Brookhart, *Organometallics* **1999**, *18*, 65−74.

[7] [7a] A. A. Paulovicova, U. El-Ayaan, K. Shibayama, T. Morita, Y. Fukuda, *Eur. J. Inorg. Chem.* **2001**, 2641−2646. [7b] A. A. Paulovicova, U. El-Ayaan, K. Umezava, C. Vithana, Y. Ohashi, Y. Fukuda, *Inorg. Chim. Acta* **2002**, *339*, 209−214. [7c] D. S. Tromp, M. A. Duin, A. M. Kluwer, C. J. Elsevier, *Inorg. Chim. Acta* **2002**, *327*, 90−97. [7d] R. J. Maldanis, J. S. Wood, A. Chandrasekaran, M. D. Rausch, J. C. W. Chien, *J. Organomet. Chem.* **2002**, *645*, 158−167. [7e] M. Gasperini, F. Ragaini, S. Cenini, *Organometallics* **2002**, *21*, 2950−2957.

[8] [8a] *Gmelin Handbook of Inorganic Chemistry, Sc, Y, La-Lu: Rare Earth Elements*, 8th Ed.; Springer-Verlag; Berlin, **1980**; Vol. D1. [8b] I. L. Fedushkin, M. N. Bochkarev, V. I. Nevodchikov, *Russ. Chem. Bull. Int. Ed.* **1995**, *44*, 2185−2186. [8c] M. N. Bochkarev, I. L. Fedushkin, V. I. Nevodchikov, V. K. Cherkasov, H. Schumann, H. Hemling, R. Weimann, *J. Organomet. Chem.* **1996**, *524*, 125−131. [8d] M. N. Bochkarev, B. I. Petrov, I. L. Fedushkin, T. V. Petrovskaya, V. I. Nevodchikov, N. B. Patrikeeva, L. N. Zakharov, Yu. T. Struchkov, *Russ. Chem. Bull. Int. Ed.* **1997**, *46*, 371−373. [8e] T. V. Petrovskaya, I. L. Fedushkin, M. N. Bochkarev, H. Schumann, R. Weimann, *Russ. Chem. Bull. Int. Ed.* **1997**, *46*, 1766−1768. [8f] T. V. Petrovskaya, I. L. Fedushkin, V. I. Nevodchikov, M. N. Bochkarev, N. V. Borodina, I. L. Eremenko, S. E. Nefedov, *Russ. Chem. Bull. Int. Ed.* **1998**, *47*, 2271−2273. [8g] H. Bock, J.-M. Lehn, J. Pauls, S. Holl, V. Krenzel, *Angew. Chem.* **1999**, *111*, 1004−1008; *Angew. Chem. Int. Ed.* **1999**, *38*, 952−955. [8h] I. L. Fedushkin, T. V. Petrovskaya, F. Girgsdies, R. D. Köhn, M. N. Bochkarev, H. Schumann, *Angew. Chem.* **1999**, *111*, 2407−2409; *Angew. Chem. Int. Ed.* **1999**, *38*, 2262−2264. [8i] I. L. Fedushkin, T. V. Petrovskaya, F. Girgsdies, V. I. Nevodchikov, R. Weimann, H. Schumann, M. N. Bochkarev, *Russ. Chem. Bull. Int. Ed.* **2000**, *49*, 1869−1876. [8j] M. Schultz, J. M. Boncella, D. J. Berg, T. D. Tilley, R. A. Andersen, *Organometallics* **2002**, *21*, 460−473. [8k] D. J. Berg, J. M. Boncella, R. A. Andersen, *Organometallics* **2002**, *21*, 4622−4631.

[9] [9a] F. G. N. Cloke, H. C. de Lemos, A. A. Sameh, *J. Chem. Soc., Chem. Commun.* **1986**, 1344−1345. [9b] A. Recknagel, M. Noltemeyer, F. T. Edelmann, *J. Organomet. Chem.* **1991**, *410*, 53−61. [9c] F. G. N. Cloke, *Chem. Soc. Rev.* **1993**, 17−24. [9d] M. N. Bochkarev, A. A. Trifonov, F. G. N. Cloke, C. I. Dally, P. T. Matsunaga, R. A. Andersen, H. Schumann, J. Loebel, H. Hemling, *J. Organomet. Chem.* **1995**, *486*, 177−182. [9e] A. Scholz, K.-H. Thiele, J. Scholz, R. Weimann, *J. Organomet. Chem.* **1995**, *501*, 195−200. [9f] A. A. Trifonov, L. N. Zakharov, M. N. Bochkarev, Yu. T. Struchkov, *Izv. Akad. Nauk, Ser. Khim* **1994**, 148−151. [9g] H. Görls, B. Neumüller, A. Scholz, J. Scholz, *Angew. Chem.* **1995**, *107*, 732−735; *Angew. Chem. Int. Ed. Engl.* **1995**, *34*, 673−676. [9h] M. Haaf, A. Schmiedl, T. A. Schmedake, D. R. Powell, A. J. Millevolte, M. Denk, R. West, *J. Am. Chem. Soc.* **1998**, *120*, 12714−12719. [9i] J. Scholz, H. Görls, H. Schumann, R. Weimann, *Organometallics* **2001**, *20*, 4394−4402.

[10] [10a] J. J. Brooks, W. Rhine, G. D. Stucky, *J. Am. Chem. Soc.* **1972**, *94*, 7346−7351. [10b] A. V. Protchenko, L. N. Zakharov, M. N. Bochkarev, Yu. T. Struchkov, *J. Organomet. Chem.* **1993**, *447*, 209−214. [10c] I. L. Fedushkin, M. N. Bochkarev, H. Schumann, L. Esser, G. Kociok-Köhn, *J. Organomet. Chem.* **1995**, *489*, 145−151. [10d] M. N. Bochkarev, I. L. Fedushkin, R. B. Larichev, *Russ. Chem. Bull. Int. Ed.* **1996**, *45*, 2443−2444. [10e] M. N. Bochkarev, I. L. Fedushkin, A. A. Fagin, H. Schumann, J. Demtschuk, *Chem. Commun.* **1997**, 1783−1784. [10f] A. V. Protchenko, O. G. Almazova, L. N. Zakharov, G. K. Fukin, Yu. T. Struchkov, M. N. Bochkarev, *J. Organomet. Chem.* **1997**, *536−537*, 457−463. [10g] M. N. Bochkarev, *Chem. Rev.* **2002**, *102*, 2089−2117.

[11] E. de Boer, *Adv. Organomet. Chem.* **1964**, *2*, 115−155.

[12] H. tom Dieck, I. W. Renk, *Chem. Ber.* **1971**, *104*, 110−130.

[13] W. von Schröter, K.-H. Lautenschläger, H. Bibrack, A. Schnabel, *Chemie*, VEB Verlag, Fachbuchverlag Leipzig, **1986**.

[14] I. L. Fedushkin, A. A. Skatova, V. A. Chudakova, G. K. Fukin, *Angew. Chem.*, in press.

[15] [15a] V. C. Gibson, J. A. Segal, A. G. P. White, D. J. Williams, *J. Am. Chem. Soc.* **2000**, *122*, 7120−7121. [15b] P. J. Bailey, R. A. Coxall, C. M. Dick, S. Fabre, S. Parsons, *Organometallics* **2001**, *20*, 798−801. [15c] P. J. Bailey, S. T. Liddle, C. A. Morrison, S. Parsons, *Angew. Chem.* **2001**, *113*, 4595−4598; *Angew. Chem. Int. Ed.* **2001**, *40*, 4463−4466. [15d] M. H. Chisholm, J. C. Huffman, K. Phomphrai, *J. Chem. Soc., Dalton Trans.* **2001**, 222−224. [15e] M. H. Chisholm, J. C. Huffman, K. Phomphrai, *Inorg. Chem.* **2002**, *41*, 2785−2794.

[16] S. Harder, *Organometallics* **2002**, *21*, 3782−3787.

[17] V. Lorenz, B. Neumüller, K.-H. Thiele, *Z. Anorg. Allg. Chem.* **1994**, *620*, 691−695.

[18] V. Lorenz, B. Neumüller, K.-H. Thiele, *Z. Naturforsch., Teil B* **1995**, *50*, 71−75.

[19] M. Rieckhoff, U. Pieper, D. Stalke, F. T. Edelmann, *Angew. Chem.* **1993**, *105*, 1102−1104; *Angew. Chem. Int. Ed. Engl.* **1993**, *32*, 1079−1081.

[20] I. L. Fedushkin, A. A. Skatova, V. A. Chudakova, V. K. Cherkasov, S. Dechert, H. Schumann, *Chem. Eur. J.*, accepted for publication.

[21] A. L. Spek, *PLATON A Multipurpose Crystallographic Tool*, Utrecht University **2000**.

[22] R. D. Shannon, *Acta Crystallogr., Sect. A* **1976**, *32*, 751−767.

[23] V. Gutmann, *Coordination Chemistry in Non-Aqueous Solutions*, **1968**, Springer-Verlag, Wien-New York, 30. Dielectric constants for THF −7.6 and pyridine −12.3.

[24] R. S. Berry, *J. Chem. Phys.* **1960**, *32*, 933−938.

[25] S. Alvarez, M. Llunell, *J. Chem. Soc., Dalton Trans.* **2000**, 3288−3303.

[26] G. M. Sheldrick, *SHELXS-97 Program for the Solution of Crystal Structures*; Universität Göttingen **1990**.

[27] G. M. Sheldrick, *SHELXL-97 Program for the Refinement of Crystal Structures*; Universität Göttingen **1997**.

[28] H. D. Flack, *Acta Crystallogr., Sect. A* **1983**, *39*, 876−881.

[29] G. M. Sheldrick, *SADABS Program for Empirical Absorption Correction of Area Detector Data*; Universität Göttingen **1996**.

Received April 1, 2003
Early View Article
Published Online August 11, 2003

